VI International Conference on Computational Methods for Coupled Problems in Science and Engineering
COUPLED PROBLEMS 2015
B. Schrefler, E. Oñate and M. Papadrakakis (Eds)

HOW THE MORPHOLOGIES OF PROGENITOR AND MATURE OSTEOCYTES CONTRIBUTES TO THEIR MECHANO-TRANSDUCTION

E. BUDYN[*], M. BENSIHOUM[†††], T. MARSAN[*], F. MANNEMARE[*], S. SASNOUSKI[†], P. TAUC[†], E. DEPREZ[†] AND H. PETITE[†††]

[*] Department of Mechanical Engineering, LMT CNRS UMR 8535
[†] Department of Biology, LBPA CNRS UMR 8113
Ecole Normale Superieure de Cachan
94230 Cachan, France
email: elisa.budyn@ens-cachan.fr, thibault.marsan@ens-cachan.fr, florian.mannemare@ens-cachan.fr, sergei.sasnouski@ens-cachan.fr, tauc@lbpa.ens-cachan.fr, deprez@lbpa.ens-cachan.fr, http://www.lmt.ens-cachan.fr

[††] Departments of Bioengineering and Orthopedic Surgery – CNRS UMR B2OA 7052
University Paris Diderot
University Paris-Sorbonne, France
email: morad.bensidhoum@paris7.jussieu.fr, herve.petite@univ-paris-diderot.fr, http://b2oa.eu/spip/

Key words: Osteocyte, bone, mechano-transduction, CFSE, h bm MSCs, MLOY4.

Abstract. A dual experimental and numerical top-down approach is applied to investigate the link between the osteocyte morphology and their mechanical perception of the environment at the progenitor and mature stages. The numerical model is based on explicit tissue morphology discretization to identify bone *in situ* diffuse damage at the cellular scale. The 3D morphology of a human mature osteocyte was reconstructed from deconvoluted confocal microscopy observations. The *in vitro* experimental model presents Live Allograft Bone Systems (LABS) where a patient progenitor (bm hMSC) or mature (MLOY4) osteocytes were reseeded into fresh human donor cortical bone tissues. The system was subjected to mechanical loading and simultaneously progenitor and mature cell specific possible calcium mediated cell signaling responses were measured by fluorescent flow cytometry using CFSE labeling.

1 INTRODUCTION

With increasing life expectancy, bone pathologies related to massive bone loss occur later in life and carry $5-$10 billion financial burden on the U.S. healthcare system. Human Haversian cortical bone is a complex hierarchical heterogeneous tissue resulting from continuous remodeling. Micro damage are therefore resorbed by osteoclasts cells before tubular lamellar structures called osteons are formed by osteoblast cells laying Type I collagen fibrils mineralized by hydroxyapatite nano-platelet crystals glued together with non-collagen proteins and proteoglycans. Trapped osteoblasts further differentiate into mechano-sensitive osteocytes that are able to sense stimulation produced by micro damage.

However bone healing ability declines with long term degeneration during aging, massive trauma or large tissue resections such as tumor removals. To promote bone growth in large defects, autograft bone offers the gold standard repair but is limited by suitable tissue quantities and donor site morbidity. Successful techniques for massive tissue regeneration can be however difficult to produce and often require addition of functional materials. Nonetheless, allograft bone can be stored but does not always perform as well as fresh allograft and the current tissue disinfection procedures such as supercritical carbon dioxide significantly modifies the tissue properties. Yet cleaned and decellularized tissue from a donor represents the ideal matrix for co-cultures of the recipient patient cells for fast tissue reintegration and functionalization [1].

Mature osteocytes have the particularity to bear 40 to 60 cytoplasmic processes extending into canaliculi to create a syncytial network with the neighboring cells with which they can transmit signals in a fashion similar to the nervous system. Because osteocytes regulate healthy bone turnover, it is essential to quantify the relationship between *in situ* mechanical stimulation and the cell biological response.

2 DESCRIPTION OF THE MODEL

2.1 Micro damage threshold identification

Dual experimental and numerical top-down investigations were applied through micro bending tests conducted on human femoral fresh cadaver samples to produce and image the growth of controlled nascent sub-microscopic damage near live osteocytes. The multi-scale local constitutive fracture mechanisms has been identified scale by scale after the balance of the energies at the global scale to evaluate the *in situ* stress field near bone cells shown in Figure 1 (a) and (B). The finite element model is based on explicit bone tissue morphology including the primary, secondary osteons and cement lines. The model Dirichlet boundary conditions are calculated by digital image correlation [2]. The osteon lamellae collagen orientations were modeled by cubic spline and crack bridging by the mineralized collagen fibers in the wake of the crack tips was modeled by a cohesive zone of 50 μm maximum length and 25 μm maximum opening from experimental measurements. The model must satisfy the macroscopic Dirichlet boundary conditions at each loading step, n. The micro damage threshold values and location were then identified by Newton-Raphson iteration algorithm on the local element elastic moduli at each macroscopic loading step and are described by the following constitutive relationship:

$$E_I^n = E_I^0(1 - d_I^n) \tag{1}$$

where E_I^n is the converged elastic moduli of element I at macroscopic loading step n, E_I^0 is the intact elastic moduli of element I prior to macroscopic loading and d_I^n is the converged microdamage parameter in element I at macroscopic load step n. The local micro damage threshold is calculated when the local maximum principal stress exceeds the identified local yield strengths, σ_y^n as follows:

$$d = \left(1 - \frac{\sigma_y^n}{\sigma^n}\right) \tag{2}$$

where σ^n is local máximum principal stress at loading step n in the intact material.

The numerical model shows nascent diffuse damage within osteon lamellae appearing in locations where visible micro cracks further appear at higher load in Figure 1 (C) and (D).

Multi-modal imaging techniques using UV and fluorescent microscopy shown in Figure 1 coupled to a hierarchical multi-level numerical simulations contributed to confirm the location of diffuse damage regions ahead of micro crack tips prior to their growth initiation [2]. Dual SEM and BSEM microscopy were applied to image the relationship between sub-micro cracks in the osteonal lamellae and the canaliculi [4].

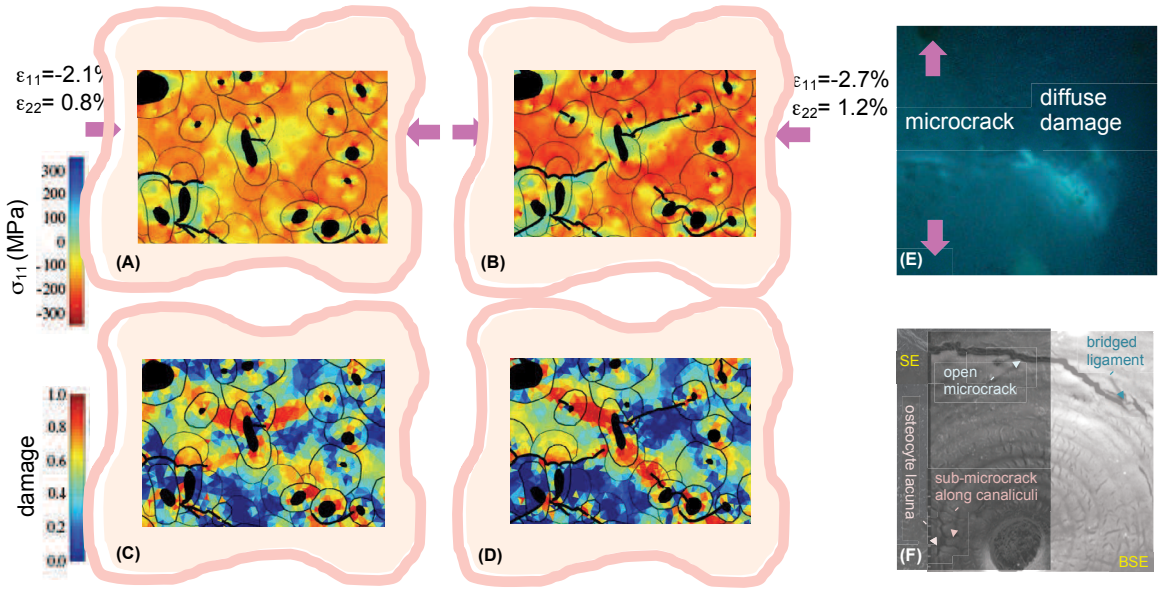

Figure 1: Diffuse damage numerical and experimental identifications in human Haversian cortical bone: (A) and (B) numerical identification of the compressive stress field before and after microcrack growth in a local FEM model including the osteon elastic moduli heterogeneity, the cohesive strength variation with the osteonal lamella orientations and mineralizations and the diffuse damage identification regularizing the local model response with the global sample response, (C) and (D) corresponding diffuse damage local identification, (E) diffuse damage visualization within the osteonal lamellae in the region of a microcrack tip using fluorescence microscopy of human cortical bone stained with calcein blue, (F) identification of sub-microcracks along osteocyte canaliculi in a region neighboring diffuse damage using superimposition of secondary electron and backscattered electron microscopy.

2.2 Three-dimensional numerical reconstruction of human osteocyte morphology

The osteocyte morphology was observed in fresh human cortical bone simple of 500 µm thickness. A osteocyte in a region containing intra-lamellar sub-micro damage is selected for confocal observation. A tissue depth of 16 µm was penetrated by two photon laser excitation in the 650 nm range that provided the best detection of the integrin proteins layer coating the osteocyte lacunae and the canaliculi in which the osteocytic processes run inside Haversian bone as shown in Figure 2-A. Resolution of 0.18 µm /px was achieved in segmentation planes

and 0.51 micron in the orthogonal direction to the planes. Due to the non-zero thickness of the confocal plane of observation, the images were deconvoluted to rebuild a cubic voxel of the 3D confocal observation of the osteocyte morphology.

The 3D morphology of the osteocytes was first reconstruction using medical image visualization software imageJ [5]. The cell body contours were digitally surveyed in the parallel segmentation planes and regularized by smoothing interpolation to remove non-physical noise perturbations. The canaliculi center paths were identified by finding the best path in 3D between points of the same canaliculus by bidirectional search A* on the reciprocal of the cost of moving to another point in the specific Fiji Plugin for cell processes tracking called Simple Neurite Tracer [6].

The complete osteocyte morphology was reconstructed in Matlab based the body contours from the 3D parallel plane segmentation and the regularized center lines of the cell processes using Tubeplot [7]. Previous osteocyte morphology reconstruction captured up to 9 cell processes [8, 9]. In the presented model, 23 processes of the osteocyte were rebuilt in Figure 2-B from the usual 40 bear by such cell.

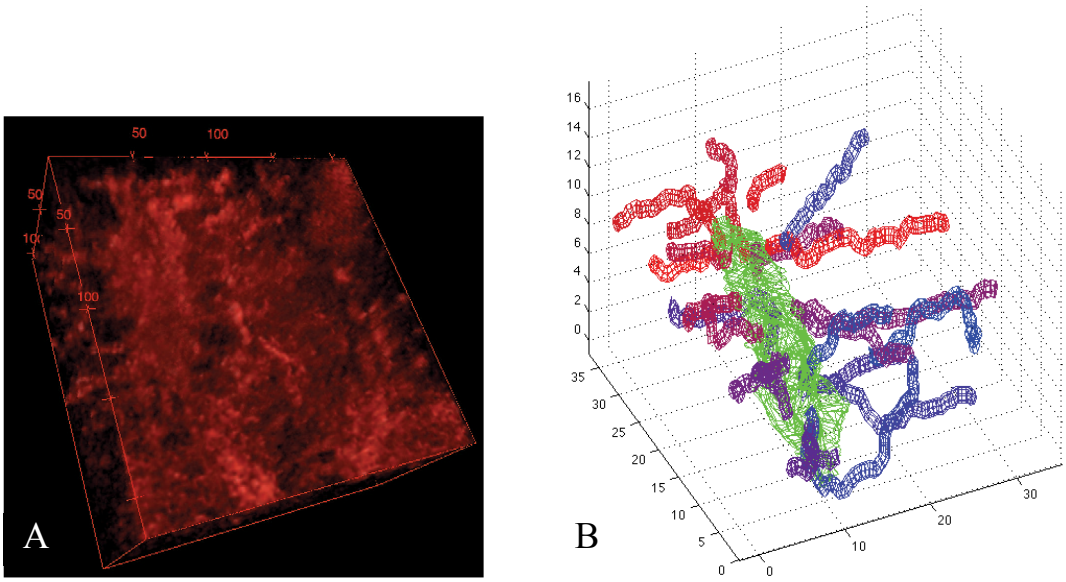

Figure 2: A- 3D confocal microscopy observation of a human osteocyte lacunae and canaliculi in fresh human Haversian cortical bone observed in the transverse direction to the osteons, B- 3D numerical reconstruction of a human osteocyte morphology from confocal microscopy observations.

2.3 Fluorescent flow cytometry in the osteocytes under mechanical loading

Osteocytes are known to respond to mechanical cues by releasing specific chemicals such as calcium [10, 11], PGE1 and NO [12] that can be observed under fluorescent microscopy by markers and are correlated to the cell biological reaction to mechanical stress. To quantify the cell morphology, displacements and *in situ* biological response, progenitor bone cells (MSC) and mature osteocytes (MLOY4) were reseeded in fresh human cortical bone tissues and observed in Nikon-Eclipse TE 200-U fluorescent microscope (B2OA Laboratory, Paris) in Figure 3 and 4 and a Nikon confocal microscope (LBPA Laboratory, Cachan) in Figure 3.

The fluorescence of the osteocytes was enhanced by labeling their cytoplasm with CFSE cell-tracker (Invitrogen). A protocol to clean fresh human bone without altering its mechanical properties was developed using a succession of baths with a solvent and a basic solution, antibiotics, trypsin and a detergent. Live cells were then reseeded in the human bone bathed in biological serum. Bone marrow human mesenchymal stem cells (bm hMSC) harvested on a patient were used for the progenitor osteocytes and mouse mature osteocyte-like cells (MLOY4) were used for mature osteocytes because of the difficulty to isolate primary human mature osteocytes. The cell suspensions (10^5 per ml) were then added to bathe the donor bone tissues. After 5 days the cells were evenly reseeded on the tissue. After 10 days progenitor and mature reseeded osteocytes reorganized as shown in Figure 3.

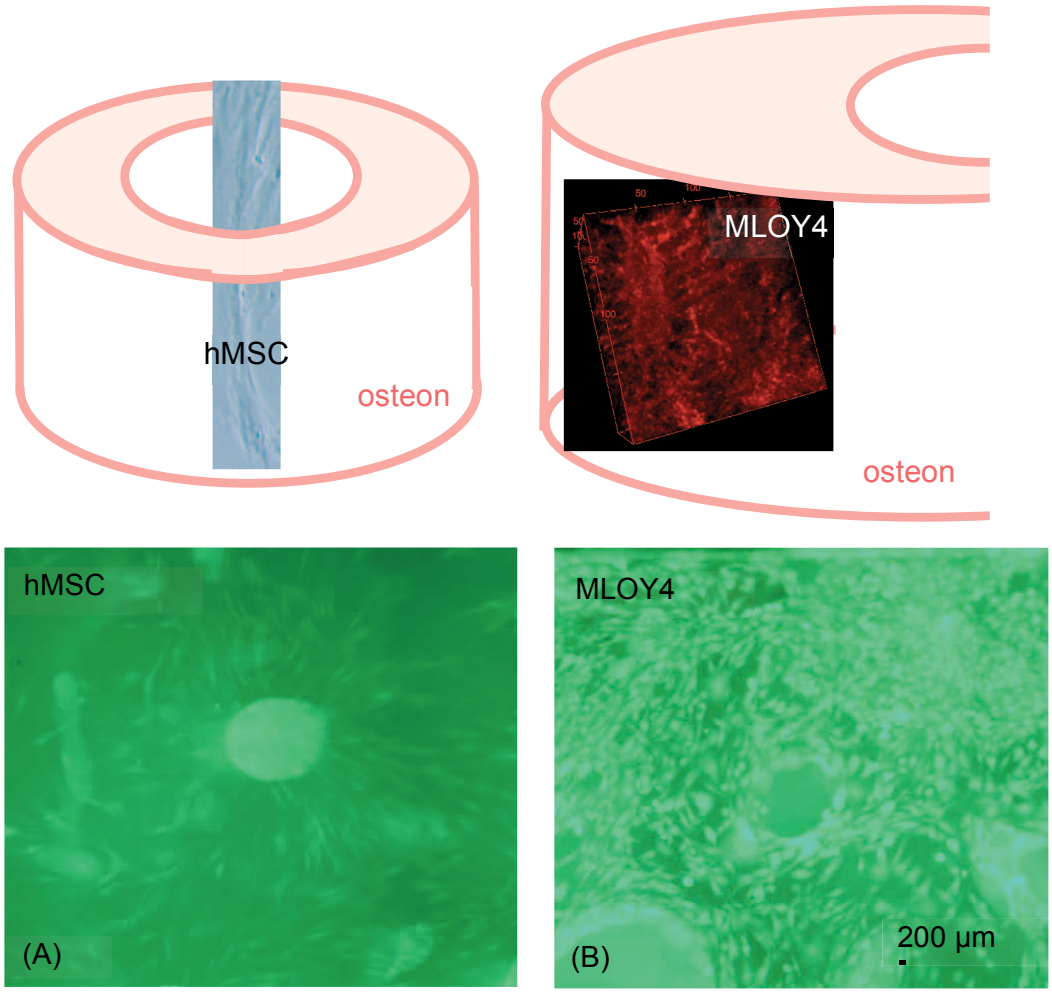

Figure 3: Cell reseeded in human Haversian cortical bone rearrangement after 10 days: (A) progenitor osteocytes (hMSC) moving into the Haversian canals and organized in radial hair-like arrays around the Haversian canals on the osteons transverse cross-section and schematic arrangement of hMSC in the Haversion canal *in vivo* presented above, (B) mature osteocytes (MLOY4) spread throughout the osteon cross-section and schematic arrangement of mature osteocyte observed under confocal microscopy in the osteonal lamellae *in vivo*.

3 RESULTS

3.1 Mechanical response of Live Allograft Bone Systems (LABS)

The numerical model identified nascent diffuse damage within osteon lamellae appearing prior to visible micro cracks as local stresses increase from yield values of 58/-77 MPa close to HAP (hydroxyapatite) strength to 108/-216 MPa when mineralized collagen fibers still bridge cracks [2]. These results confirm known brittle/ductile fracture behavior of bone through load bearing cooperation between HAP mineral phase and organic collagen fibers.

Multi-modal SEM and BSEM microscopic observations within osteon lamellae showed micro-damage patterns near osteocytic processes and canaliculi in Figure 1 (F) in regions neighboring a visible micro cracks and containing diffuse damage. Calcein blue staining of cortical bone reveals diffuse damage regions in Figure 1 (E) where calcium ions exposed on hydroxyapatite broken edges interact with the stain [13].

The load deflection curves of the recellularized bone tissues are shown in Figure 4 for the allograft bone systems containing either bm hMSC or MLOY4 and tested in the elastic region prior to visible micro crack initiation but containing diffuse damage [13] in the anti-plane longitudinal direction. The mechanical responses of the Live Allograft Bone Systems (LABS) were compared to the mechanical responses of fresh cadaver human bone tissues samples tested until complete failure in the three characteristic directions of the osteons.

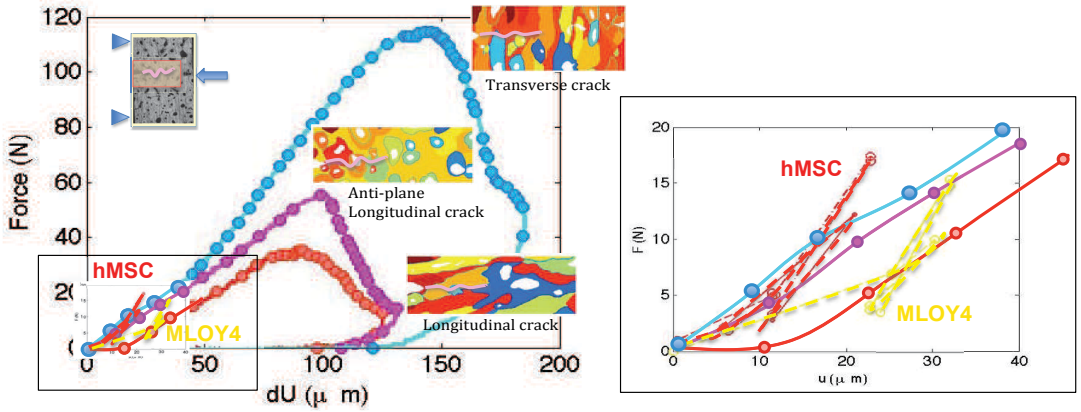

Figure 4: Load-deflection curves of micro 3-point bending tests of fresh cadaver human cortical bone samples in the longitudinal, anti-plane longitudinal and transverse directions until complete fracture compared to micro 3-point bending tests of anti-plane longitudinal human cortical bone samples that are recellularized with either progenitor or mature osteocytes and loaded in the elastic region prior to fracture.

3.2 Progenitor and mature osteocyte *in vitro* special reorganizations on bone tissue

bm hMSCs and MLOY4 cells reorganized *in vitro* as they would *in vivo* in fresh donor bone tissue as shown in Figure 3 after 10 days in an incubation chamber at 37°C. After 10 days incubation, reseeded MCSs relocated inside the Haversian canals in the human tissue samples. The elongated MSCs cells are located *in vivo* in the bone marrow and circulate inside the Haversian canals of cortical bone. MCSs also exhibit morphological features with strong affinities to the topography of their residing lodges. On the other had after 10 days, mature osteocytes seeded and proliferated on the solid osteonal lamellae structures with

characteristic spacing observed in bone osteocyte lacunae organization. The osteocytes also regained hedgehog-like shapes and spread osteocytic processes to recreate a syncytial network as *in vivo*. Progenitor and mature osteocytes reseeded in cortical bone tissues therefore reconstituted live allograft bone systems similar to *in vivo* systems.

3.3 Progenitor and mature osteocyte biological responses to mechanical loading

The osteocyte biological response to mechanical loading was visualized by the instantaneous variation of fluorescence intensity due to cytoplasm staining by CFSE cell tracker. CFSE is a small molecule of 0.473 kDa molecular mass, that is easily permeable to cell plasma membrane in the form of CFDA-SE that looses its diacetate group through an intracellular esterase to become CFSE that covalent binds to intracellular Lysine residues of intracellular proteins and amines. CFSE is a biochemical dye to track cell proliferation over multiple days and also indicates cell viability when used in short amount of time. CFSE and Fluo4-AM labeling have also been used together to track lymphocyte proliferation and measure cytosolic free calcium simultaneously [14]. Figure 4 shows that bm hMSCs lost suddenly their fluorescence under mechanical loading less than 21 N while osteocytes retains a significant amount of fluorescence in Figure 5 for larger mechanical loading-unloading increment cycles up to 147 N shown in Figure 4. However, at larger loading increment despite almost no fluorescence, high magnification reveal that the bm hMSCs contours are still perceivable which could indicate that the cell integrity are preserved and that the cells did not loose fluorescence by plasma membrane rupture but possible other cell signaling mechanisms.

CFSE binds to Lysine and Lysine is an essential α-amino acid that plays a role in different posttranslational modifications such as methylation of the ε-amino group into methyl-, dimethyl- and trimethyllysine that occurs in calmodulin. Calmodulin (CaM for Calcium-Modulated proteIn) is a calcium-binding multifunctional intermediate messenger protein that transduces calcium signals by binding calcium ions and modify its interactions to target proteins afterwards. Proteins that bind to CaM cannot bind to calcium and uses CaM as a calcium sensor and a signal transducer. Calmodulin 1 in particular is located in the cytosol and on the plasma membrane facing the cytosol, CALM1 interacts with cation channel receptors such as TRPV1 activated in the sensation of pain. Calmodulin also mediates processes such as inflammation and apoptosis. L-Lysine plays therefore a very important role in calcium absorption.

Lysine also plays a role in posttranslational modifications such as neddylation, biotinylation, pupylation and carboxylation but most importantly in acetylation, sumoylation, ubiquitination involved in apoptosis and cell response to stress. CFSE binds to lysine through an esterase that operates a deacetylation of CFDA-SE. Acetylation and deacetylation of a protein are significant posttranslational regulatory mechanisms that occur in the regulation of transcription factors, effector proteins, molecular chaperones and cytoskeletal proteins in an analogous manner to phosphorylation and dephosphorylation under the action of kinases and phosphatases. Acetylation and deacetylation has been suggested to crosstalk with key other biological mechanisms such as phosphorylation, methylation, ubiquitination, sumoylation [15] and different cell signaling such as the synthesis of tubulin of the microtubules of the cytoskeleton in which lysine take part and are solicited under mechanical load.

For all the above possible cell mechanisms' interactions and from previous experiments on cell CFSE labeling and calcium flow cytometry [14] and experiments on osteocytes and osteoblasts calcium different responses [16], it is hypothesized that CFSE labeling is indicative here of distinct calcium responses from bone stromal cells at their progenitor and mature stages of their differentiation shown in Figure 5.

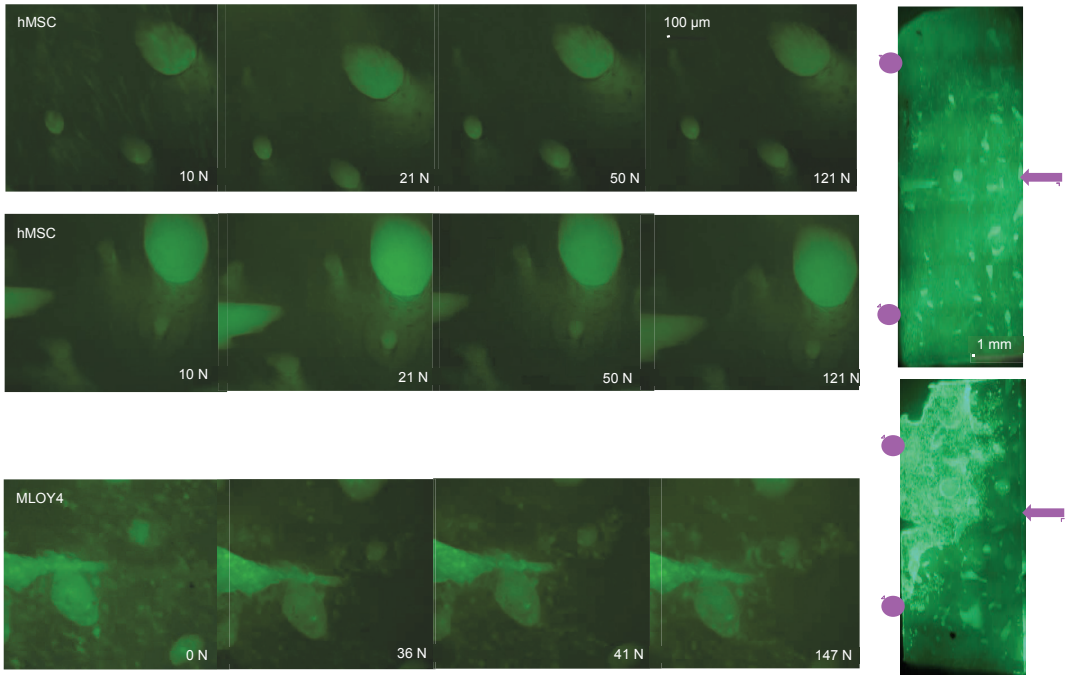

Figure 5: Fluorescence decreasing of the cytoplasm of hMSC and MLOY4 cells stained with CFSE cell tracker when subjected to increasing tensile loading produced by the tension in the human Haversian cortical bone environmental "substrate".

4 CONCLUSIONS

Hybrid experimental and numerical investigations quantified human osteocyte lacunae and canaliculi morphology alterations in bone diffuse damage areas that were correlated to nascent sub-micro cracks. Figure 4 showed the mechanical responses of live allograft bone systems containing live osteocytes that were consistent with the known mechanical response of fresh cadaver human bone tissue. Figure 3 reveals distinct spatial reorganizations of progenitor osteocytes in the Haversian canals after 10 days from the rearrangement of mature osteocytes regularly dispersed throughout the osteonal lamellae after 10 days of incubation. After 10 days the cells relocated in the allograft tissue microstructure studied here *in vitro* as they would be located *in vivo*: progenitor cells in the Haversian canals and mature osteocytes within the mineralized osteonal solid matrix. Human bone marrow mesenchymal stem cells also exhibited a typical elongated tubular shape and migrated into tubular Haversian canals while mature osteocytes displayed oblate-shaped bodies bearing multiple processes acting as hair-like structures shown in Figure 2 to detect mechanical loading in the mineralized extracellular matrix [17]. Loss of fluorescence shown in Figure 5 could be correlated to

possible calcium mediated cell signaling mechanisms involving lysine residues to which CFSE stain binds under the plasma membrane facing cytosolic free calcium participating into efflux through cytoplasmic membrane pumps or intracellular recycling. This aspect is currently under further investigations. Mesenchymal stem cells lost fluorescence under very low loading while a non-negligible percentage of the mature osteocytes retained some fluorescence at moderated load in Figure 5 that is in agreement with a modified calcium response of osteocytes through their differentiating stages observed in the literature [16].

ACKNOLEDGMENT

The authors are grateful to the support of the Farman Institute for the project OLA!. The first author is extremely grateful for the generous support from CMMI BMMB NSF program for Grant 1214816.

REFERENCES

[1] Nather, A., David, V., Teng, J.H.W., Lee, C.W., and Pereira, B.P. Effect of autologous mesenchymal stem cells on biological healing of allografts in critical-sized tibial defects simulated in adult rabbits. *Annals Academy of Medicine* (2010) **39**(8):599-606.

[2] Jonvaux, J., Hoc, T., and Budyn, E. Analysis of micro fracture in human Haversian cortical bone under compression. *International Journal for Numerical Method in Biomedical Engineering* (2012) **28**(9):974-998.

[3] E. Budyn and T. Hoc, Analysis of micro fracture in human Haversian cortical bone under transverse tension using extended physical imaging. *International Journal for Numerical Method in Engineering* (2010) **82**(8):940-965.

[4] Wang, Y., McNamara, L.M., Schafler, M.B., and Weinbaum, B. Strain amplification and integrin based signaling in osteocytes. *J. Musculoskelet. Neuronal Interact* (2008) **8**(4):332-334.

[5] Rasband, W. National Institue of Health. http://imagej.nih.gov/ij/

[6] Longair, M.H., Baker, D.A., and Armstrong, J.D. Simple Neurite Tracer: Open Source software for reconstruction, visualization and analysis of neuronal Processes. *Bioinformatics Advance Access*. (2011).

[7] Weisenberg, J.H. TubePlot. (2004) http://www.mathworks.com/matlabcentral/fileexchange/5562-tubeplot

[8] Stern-Rath A. and Nicolella D.P., Measurement and estimation of osteocyte mechanical strain. *Bone* (2013) **54**:191-195.

[9] Verbruggen, S.W., Vaughan, T.J., McNamara, L.M. Fluid flow in the osteocyte mechanical environment : a fluid–structure interaction approach. *Biomechanical Modelling in Mechanibiology* (2014) **13**:85-97.

[10] Rawlinson, S.C.F., Pitsillides, A.A. and Lanyon L.E. Involvement of different ion channels in oseoblasts' and osteocytes, early responses to mechanical strain, *Bone* (1996) **19**(6):609-614.

[11] Huo, B., Lu, X.L., Costa, K.D., Xu Q. And Guo X.E. An ATP-dependent mechanism mediates intracellular calcium signaling in bone cell network under single cell

nanoidentation. *Cell Calcium* (2010) **47**:234-241.

[12] Kitase, Y., Van Der Plas, A., Semeins, C.M., Ajubi, N.E., Frangos, J.A., Nijweide, P.J. and Burger, E.H.. Mechanical induction of PGe2 in osteocytes blocks glucocorticoid-induced apoptosis through both the beta-catenin and PKA pathways. *Journal of Bone Mineral Research* (2010) **25**(12):2657-2668.

[13] Sun, X., McLamore, E., Kishore, V., Slipchenko, M., Porterfield, D.M. and Akkus, O. Mechanical stretch induced calcium efflux from bone matrix stimulates osteoblasts. *Bone* (2012) **50**:581-591.

[14] Mukherjee, M.S., Giamberardino, C., Thomas, J., Evans, K., Goto, H., Ledford, J.G., Hsia, B., Pastva, A.M. and Wright J.R. Surfactant protein A integrates activation signal strength to differentially modulate T cell proliferation. *The Journal of Immunology* (2012) doi:10.4049/jimmunol.1100461.

[15] Yang, X.J. and Seto E. Lysine acetylation: codified crosstalk with other posttranslational modifications. *Molecular Cell* (2008) **31**:449-461.

[16] Lu, X.L., Huo, B., Chiang V. and Guo X.E. Osteocytic network is more responsive in calcium signaling that osteoblastic network under fluid flow. *Journal of Bone Mineral Research* (2012) **27**(3):563-574.

[17] Budyn, E., Tauc, P., Bensidhoum, M., Petite, H. and Deprez, E. Back to life: fresh osteocytes spreading their processes for optimum mechanotransduction near micro damage in dead bone. *Medical Engineering Centres Annual Meeting and Bioengineering14*, MECbioeng14 Imperial College London, England, UK, ISBN 978-0-9930390-0-3, (2014) p.63.